

Anisotropic electrodynamics of layered metal 2H-NbSe₂

S. V. Dordevic,* D. N. Basov, and R. C. Dynes

Department of Physics, University of California, San Diego, La Jolla, California 92093

E. Bucher†

Lucent Technologies, Murray Hill, New Jersey 07974

(Received 13 June 2001; published 28 September 2001)

We have performed both in-plane and out-of-plane infrared reflectance measurements on the layered metal 2H-NbSe₂, in a broad frequency and temperature range. The electrodynamic response for both polarizations is characterized by a well-defined Drude-like absorption. The absolute values of the in-plane scattering rate are in accord with what is expected from Landau's Fermi-liquid theory, despite the fact that the functional form of $1/\tau_{ab}(\omega)$ differs from canonical ω^2 -dependence. Analysis of the scattering rate tensor is suggestive of strong anisotropy of the electron-phonon coupling constant.

DOI: 10.1103/PhysRevB.64.161103

PACS number(s): 71.45.Lr, 78.20.-e, 74.25.Gz

Transition metal dichalcogenides 2H-TMX₂, with TM = Nb, Ta, Ti, Mo, etc. and X = S, Se, Te have been a subject of continued interest because of a variety of different ground states these systems reveal depending on TM and X.¹ Renewed attention to superconducting dichalcogenides such as 2H-NbSe₂, 2H-TaS₂, and 2H-NbS₂ comes from their similarity with high transition temperature superconductors (cuprates).²⁻⁷ In both classes of materials layered structure gives rise to highly anisotropic physical properties, both above and below the superconducting transition temperature T_c. Unlike cuprates, whose interlayer c-axis transport is highly incoherent,⁸ 2H-NbSe₂ is believed to be a canonical example of a layered metal with a cylindrical Fermi surface and coherent interplane transport.⁹ Infrared studies of its conductivity tensor presented here indeed confirm the existence of well-defined quasiparticles. However, the power law of the frequency dependence of the scattering rate $1/\tau(\omega)$ is different from a Landau Fermi liquid (LFL) ω^2 form. Analysis of anisotropic carrier dynamics unveils significant electron-phonon contribution to the inelastic scattering processes.

High quality single crystals of 2H-NbSe₂ were grown at Lucent Technologies, using iodine vapor transport.¹⁰ The inset of Fig. 1 shows the temperature dependence of the in-plane DC resistivity ρ_{DC} . The resistivity is monotonic and approximately linear in T, with the onset of superconductivity around T_c = 7.2 K. The residual resistivity ratio $\rho(300\text{K})/\rho(T_c) \approx 30$ is comparable with previous reports for the best available samples.⁹ At 33 K 2H-NbSe₂ undergoes a second-order phase transition to an incommensurate charge density wave (CDW) state.¹¹ The transport properties are only weakly affected by the CDW transition. The CDW incommensurability decreases with temperature but never vanishes, and below T_c = 7.2 K superconducting and CDW states coexist.

The electronic structure and charge dynamics of 2H-NbSe₂ have been studied using polarized infrared reflectance spectroscopy and optical ellipsometry. Our experimental setup for spectroscopy of microcrystals¹² allowed us to measure the far-infrared part of the spectrum. Near-normal-incidence reflectance $R(\omega)$ of 2H-NbSe₂ single crystals was

obtained in the frequency range between 30–20 000 cm⁻¹ (3 meV - 2.5 eV). We emphasize that all measurements were performed on fresh, as-grown surfaces, which rules out extrinsic effects due to polishing. The complex conductivity $\sigma(\omega) = \sigma_1(\omega) + i\sigma_2(\omega)$ was inferred from $R(\omega)$ using Kramers-Kronig (KK) analysis. Reflectance measurements were supplemented by spectroscopic ellipsometry, performed in the frequency range 5 000–36 000 cm⁻¹ (0.5–4 eV). Ellipsometry measurements directly yield both the real and imaginary parts of the optical constants without the need for KK analysis. Excellent agreement between reflectance and ellipsometric data in the overlapping region (5 000–20 000

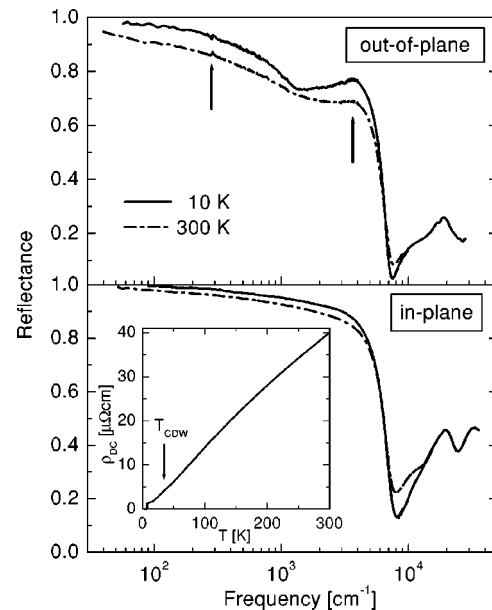


FIG. 1. Top panel: Reflectance spectra on 2H-NbSe₂ at 10 K and 300 K for the out-of-plane polarization (electric-field vector oriented perpendicular to the planes $\mathbf{E} \parallel \mathbf{c}$). Bottom panel: the spectra for the in-plane polarization (electric-field vector parallel to the planes $\mathbf{E} \parallel \mathbf{ab}$). The overall shape of reflectance is metallic for both directions. The arrows point to an infrared-active phonon and a low-lying electronic excitation (see text). The inset shows the temperature dependence of the in-plane resistivity ρ_{DC} .

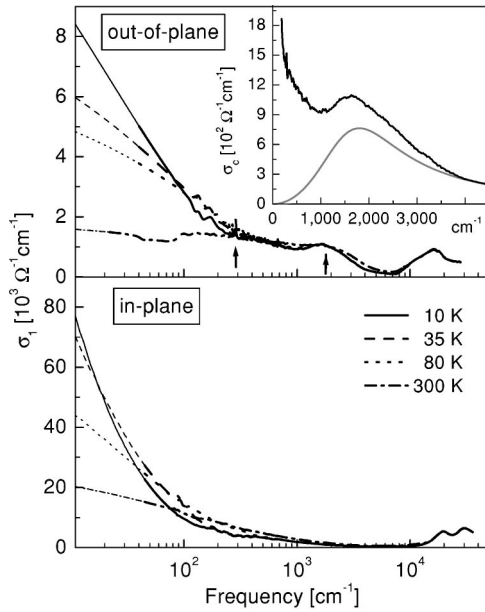


FIG. 2. Real part of the optical conductivity for both out-of-plane (top panel) and in-plane (bottom panel) directions, as obtained from KK analysis of the reflectance, at different temperatures. Thick lines are used for the measured frequency region and thin ones for the extrapolated region. The inset shows $\sigma_c(\omega)$ for the out-of-plane direction on a linear scale. The gray line is the Lorentzian oscillator representation of the 220 meV feature.

cm^{-1}) indicates that our KK analysis is reliable.

The top panel of Fig. 1 shows the out-of-plane (electric-field vector oriented perpendicular to the planes $\mathbf{E}\parallel\mathbf{c}$) and the bottom panel shows the in-plane (electric-field vector parallel to the planes $\mathbf{E}\parallel\mathbf{ab}$) reflectivity data. Only 300 K and 10 K curves are displayed for clarity. Note that the measured frequency interval extends below the CDW gap $\Delta_{CDW} = 35 \text{ meV} \approx 280 \text{ cm}^{-1}$ obtained by tunneling experiments.¹³ The overall behavior of $R(\omega)$ is metallic in both directions, with clearly defined plasma edges around 8000 cm^{-1} . The anisotropy in reflectance persists up to very high frequencies, consistent with earlier reports.¹⁴

The real part of the optical conductivity $\sigma_1(\omega)$ for both polarizations is shown in Fig. 2. The conductivity is metallic, characterized by a zero-energy peak that narrows with decreasing temperature. Several interband transitions can be identified in the range between $10000\text{--}40000 \text{ cm}^{-1}$ (see Ref. 14 for detailed analysis of interband absorption). We also note that the absolute values of $\sigma_1(\omega)$ in the region $\omega \rightarrow 0$ are typically an order of magnitude higher for the in-plane direction. No qualitatively new features, in particular no signs of a gap (i.e., suppression of conductivity at some finite frequency), can be observed at $T < T_{CDW}$. However, this is not unexpected for a two-dimensional CDW material, such as 2H-NbSe_2 . In one-dimensional systems Fermi-surface nesting is perfect, and as a result the CDW instability almost inevitably leads to the opening of a complete gap in the density of states.¹⁵ However in 2D perfect nesting is no longer possible,¹⁵ resulting in a CDW gap that affects only a small portion of the Fermi surface.^{13,16} A similar conclusion has been reached for 2H-TaSe_2 (Ref. 2), even though the

CDW instability seems to have a stronger impact on the electronic properties in this system, as indicated by a sharp drop in the resistivity below T_{CDW} .

In addition to the smooth electronic background the out-of-plane optical conductivity reveals a well-defined excitation at $\omega \approx 1800 \text{ cm}^{-1} \approx 220 \text{ meV}$ (see inset of Fig. 2). This feature may be related to a broad peak detected in photoemission spectra at the same energy and assigned to saddle points.^{3,17} A similar structure is also observed in the optical spectra of 2H-TaSe_2 at a somewhat higher frequency.⁵ An infrared-active phonon polarized in the out-of-plane direction can also be seen in the spectra at 288 cm^{-1} , with no detectable temperature shifts.

Although the optical conductivity is metallic for both polarizations, a more detailed examination of $\sigma_1(\omega)$ suggests that its frequency dependence differs from the Lorentzian form prescribed by the Drude theory. Experimentally these deviations are best resolved within the so-called “extended” Drude formalism.^{18,19} In this approach one inverts the Drude formula to determine the frequency dependence of the scattering rate:

$$\frac{1}{\tau(\omega)} = \frac{\omega_p^2}{4\pi} \text{Re} \left[\frac{1}{\sigma(\omega)} \right]. \quad (1)$$

In Eq. (1) the plasma frequency $\omega_p = \sqrt{4\pi n e^2 / m^*}$ (n is the carrier density and m^* their effective mass) can be obtained from the integration of the optical conductivity $\sigma_1(\omega)$ up to the frequency corresponding to the onset of interband absorption:

$$\omega_p^2 = 8 \int_0^W \sigma_1(\omega) d\omega. \quad (2)$$

For both polarizations $W \approx 8000 \text{ cm}^{-1}$. From Eq. (2) the following values of the plasma frequency are obtained: $\omega_p^{ab} = 21880 \text{ cm}^{-1}$ and $\omega_p^c = 9760 \text{ cm}^{-1}$ (Ref. 20). These values of plasma frequency determine the anisotropy of the effective-mass tensor $m_c^* / m_{ab}^* \approx 5$.

The top panel of Fig. 3 shows the results of the scattering rate analysis [Eq. (1)] for the out-of-plane direction. At low temperature we observe a characteristic suppression of $1/\tau_c(\omega)$ below $\sim 300 \text{ cm}^{-1}$. Above 300 cm^{-1} the scattering rate $1/\tau_c(\omega)$ saturates to a constant value. At higher temperature the low-energy feature in the $1/\tau_c(\omega)$ spectrum smears out. One can also notice an offset between the 10 K and 300 K spectra that is nearly constant at $\omega > 300 \text{ cm}^{-1}$. All these effects are consistent with the behavior of the scattering rate expected within the electron-phonon coupling theory.^{18,21–23} Further support for the latter claim comes from the Eliashberg analysis of the $1/\tau(\omega)$ data using the spectral function $\alpha^2 F(\omega)$ from Ref. 24. Within this model the frequency dependent scattering rate is expressed as:²¹

$$\frac{1}{\tau(\omega)} = \frac{2\pi}{\omega} \int_0^\infty d\Omega (\omega - \Omega) \alpha^2 F(\Omega) + \frac{1}{\tau_{imp}}, \quad (3)$$

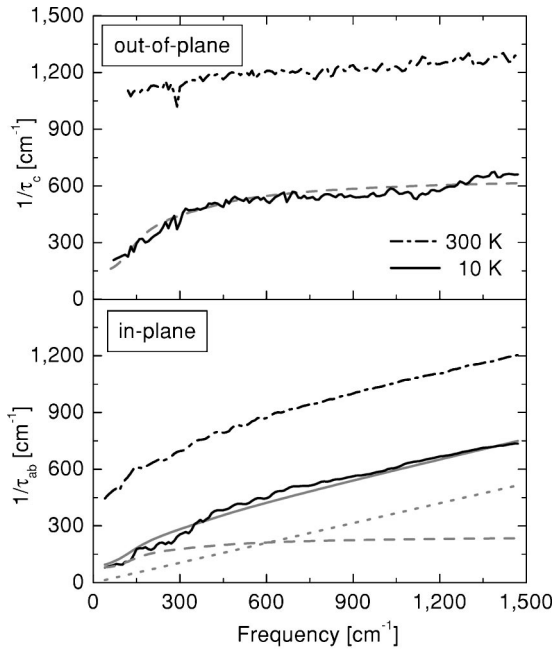


FIG. 3. The scattering rates $1/\tau(\omega)$ calculated from Eq. (1), and fits (gray lines) based on the electron-phonon spectral function [Eq. (3)]. For $1/\tau_{ab}(\omega)$ a component linear in frequency must be added (see text).

where $1/\tau_{imp}$ is the impurity scattering. The best fit (dashed gray line in Fig. 3) is obtained if the electron-phonon coupling constants $\lambda = 2 \int_0^\infty d\omega \alpha^2 F(\omega)/\omega \approx 1.59$ is used.

The bottom panel of Fig. 3 shows the in-plane scattering rate $1/\tau_{ab}(\omega)$. One notices similarities, but also some important differences with the data for the out-of-plane direction: $1/\tau_{ab}(\omega)$ is also suppressed below $\sim 300 \text{ cm}^{-1}$ (Ref. 25), but does not saturate at higher frequencies. These findings indicate that the Eliashberg theory alone is insufficient to quantitatively describe the in-plane data. Because the electron-phonon contribution to $1/\tau_{ab}(\omega)$ (dashed gray line) tends to saturate above the cut-off frequency of the phonon density of states, an additional component, approximately linear in frequency (dotted gray line) has to be added to successfully fit the data. The full gray line is the sum of linear and electron-phonon contribution for $\lambda_{ab} = 0.53$. Therefore this analysis indicates that the contribution of the electron-phonon interaction is weaker in the planes. The anisotropy of λ is known to originate from correlations between the electron group velocity and the electron-phonon matrix elements [see Eq. (10) in Ref. 26]. Based on the Fermi-surface topology of 2H-NbSe₂ (Ref. 9), the large anisotropy of λ is therefore not unexpected.

A similar linear component in the in-plane scattering rate has also been found in other 2D conductors, including 2H-

TaSe₂ (Refs. 2,4), graphite²⁷ and a number of cuprates.¹⁸ The linear scattering rate deviates from the electron-electron LFL form $1/\tau(\omega) \sim \omega^2$ observed in simple 3D metals, such as cerium,²⁸ molybdenum,²⁹ and chromium.^{30,31} However theoretical calculations^{32,33} indicate that a quasi-2D electron gas is expected to show $1/\tau(\omega) \sim \omega$ dependence. The important difference between 2H-NbSe₂ and cuprates is the absolute values of $1/\tau_{ab}(\omega)$. As can be seen from Fig. 3 in 2H-NbSe₂ at 10 K $1/\tau_{ab}(\omega)$ is always smaller than the corresponding energy: $1/\tau_{ab}(\omega) \leq \omega$. Small absolute values of $1/\tau_{ab}(\omega)$ imply that the quasiparticles in 2H-NbSe₂ are well defined, i.e., their lifetime is sufficiently long so that they can propagate coherently many interatomic distances both along and across the layers. Estimates based on both 3D and 2D free-electron gas give the in-plane mean-free-path of $\sim 100 \text{ \AA}$. A 3D estimate for the out-of-plane mean free path gives $\sim 20 \text{ \AA}$. The latter result is in full accord with de Haas-van Alphen measurements⁹ that found a 3D Fermi surface in 2H-NbSe₂.

Finally, infrared studies of the electrodynamic response of 2H-NbSe₂ allow us to comment on the origins of anisotropy in the DC transport in this system.³⁴ Quick inspection of Fig. 2 signals that both plasma frequency ω_p (area under $\sigma_1(\omega)$ curve) and carrier scattering rate $1/\tau$ (the width of zero-energy peak) contribute to the DC anisotropy. In the DC limit ($\omega \rightarrow 0$) room-temperature out-of-plane scattering rate $1/\tau_c(\omega \rightarrow 0) = 1050 \text{ cm}^{-1}$ is ~ 2.45 times greater³⁵ than in the plane $1/\tau_{ab}(\omega \rightarrow 0) = 430 \text{ cm}^{-1}$. From the Drude formula $\sigma_{DC} = \omega_p^2 \tau / 4\pi$ it follows that in the zero-frequency limit $\omega \rightarrow 0$:

$$\frac{\sigma_{ab}}{\sigma_c} = \left(\frac{\omega_p^{ab}}{\omega_p^c} \right)^2 \frac{\tau_{ab}}{\tau_c} \approx 12, \quad (4)$$

in full agreement with the room-temperature data. At low temperature the anisotropy stays roughly the same.

In conclusion, the results on the electrodynamic response on 2H-NbSe₂ presented here are suggestive of an anisotropic electron-phonon coupling constant. The in-plane scattering rate is found to be in the Landau Fermi liquid regime, indicating the existence of well-defined quasiparticles. Similar to other 2D conductors, the frequency dependence of $1/\tau(\omega)$ in 2H-NbSe₂ reveals significant linear contribution. Both the plasma frequency and the scattering rate are found to contribute to the anisotropy of the DC resistivity.

We thank P.B. Allen, L. Degiorgi, and E.J. Singley for useful discussions. The research at UCSD was supported by the U.S. Department of Energy under Grant No. DE-FG03-86ER-45230, the U.S. National Science Foundation under Grant No. DMR-98-75-980.

*Electronic address: sasa@physics.ucsd.edu

†Also at Fakultät für Physik, Universität Konstanz, D-78457 Konstanz, Germany.

¹R. L. Withers and J. A. Wilson, J. Phys. C **19**, 4809 (1986).

²V. Vescoli, L. Degiorgi, H. Berger, and L. Forro, Phys. Rev. Lett. **81**, 453 (1998).

³Th. Straub, Th. Finteis, R. Claessen, P. Steiner, S. Hufner, P. Blaha, C. S. Oglesby, and E. Bucher, Phys. Rev. Lett. **82**, 4504

- (1999).
- ⁴T. Valla, A. V. Fedorov, P. D. Johnson, J. Xue, K. E. Smith, and F. J. DiSalvo, *Phys. Rev. Lett.* **85**, 4759 (2000).
 - ⁵B. Ruzicka, L. Degiorgi, H. Berger, R. Gaal, and L. Forro, *Phys. Rev. Lett.* **86**, 4136 (2001).
 - ⁶A. H. Castro Neto, *Phys. Rev. Lett.* **86**, 4382 (2001).
 - ⁷W. C. Tonjes, V. A. Greanya, R. Liu, C. G. Olson, and P. Molinie, *Phys. Rev. B* **63**, 235 101 (2001).
 - ⁸S. L. Cooper and K. E. Gray, in *Physical Properties of High-Temperature Superconductors IV*, edited by D. M. Ginsberg (World Scientific, Singapore, 1994), pp. 61–188.
 - ⁹R. Corcoran, P. Meeson, Y. Onuki, P.-A. Probst, M. Springford, K. Takita, H. Harima, G. Y. Guo, and B. L. Gyorffy, *J. Phys.: Condens. Matter* **6**, 4479 (1994).
 - ¹⁰C. S. Oglesby, E. Bucher, C. Kloc, and H. Hohl, *J. Cryst. Growth* **137**, 289 (1994).
 - ¹¹D. E. Moncton, J. D. Axe, and F. J. DiSalvo, *Phys. Rev. B* **16**, 801 (1977).
 - ¹²S. V. Dordevic, N. R. Dilley, E. D. Bauer, D. N. Basov, M. B. Maple, and L. Degiorgi, *Phys. Rev. B* **60**, 11 321 (1999); C. C. Homes, M. A. Reedyk, D. A. Crandels, and T. Timusk, *Appl. Opt.* **32**, 2976 (1993).
 - ¹³H. F. Hess, R. B. Robinson, R. C. Dynes, J. M. Valles, and J. V. Waszczak, *J. Vac. Sci. Technol.* **8**, 450 (1990); C. Wang, B. Giambattista, C. G. Slough, R. V. Coleman, and M. A. Subramanian, *Phys. Rev. B* **42**, 8890 (1990).
 - ¹⁴W. Y. Liang, *J. Phys. C* **6**, 551 (1973); R. Bachmann, H. C. Kirsch, and T. H. Geballe, *Solid State Commun.* **9**, 57 (1971); S. S. P. Parkin and A. R. Beal, *Philos. Mag. B* **42**, 627 (1980).
 - ¹⁵G. Gruner, *Density Waves in Solids* (Addison-Wesley, Reading, MA, 1994).
 - ¹⁶A. W. McConnell B. P. Clayman, C. C. Homes, M. Inoue, and H. Negishi, *Phys. Rev. B* **58**, 13 565 (1998).
 - ¹⁷This feature is present even at room temperature and therefore not related to the CDW transition.
 - ¹⁸For a review see: A. V. Puchkov, D. N. Basov, and T. Timusk, *J. Phys.: Condens. Matter* **8**, 10 049 (1996).
 - ¹⁹J. W. Allen and J. C. Mikkelsen, *Phys. Rev. B* **15**, 2952 (1977).
 - ²⁰Determination of $1/\tau(\omega)$ and ω_p for the out-of-plane direction is more complicated because of the 220 meV feature which must be separated from the intraband contribution. For this purpose we fitted the 220 meV peak with a Lorentzian oscillator (positioned at $1,800\text{ cm}^{-1}$ with the width of $2,200\text{ cm}^{-1}$ and strength $6,000\text{ cm}^{-1}$; gray line in the inset of Fig. 2), and subtracted it from the optical conductivity.
 - ²¹P. B. Allen, *Phys. Rev. B* **3**, 305 (1971).
 - ²²J. P. Carbotte, *Rev. Mod. Phys.* **62**, 1027 (1990).
 - ²³S. V. Shulga, O. V. Dolgov, and E. G. Maksimov, *Physica C* **178**, 266 (1991).
 - ²⁴K. Motizuki, Y. Nishio, M. Shirai, and N. Suzuki, *J. Phys. Chem. Solids* **57**, 1091 (1996).
 - ²⁵The frequency below which $1/\tau_{ab}(\omega)$ is suppressed is closed to the $\Delta_{CDW}=280\text{ cm}^{-1}$ found in tunneling measurements.¹³ However we believe that this suppression is not related to the CDW transition because it exists even at room temperature.
 - ²⁶Anisotropic electron-phonon coupling constants are discussed in: B. A. Sanborn, P. B. Allen, and D. A. Papaconstantopoulos, *Phys. Rev. B* **40**, 6037 (1989).
 - ²⁷S. Xu, J. Cao, C. C. Miller, D. A. Mantell, R. J. D. Miller, and Y. Gao, *Phys. Rev. Lett.* **76**, 483 (1996).
 - ²⁸J. W. van der Eb, A. B. Kuz'menko, and D. van der Marel, *Phys. Rev. Lett.* **86**, 3407 (2001).
 - ²⁹T. Valla, A. V. Fedorov, P. D. Johnson, and S. L. Hulbert, *Phys. Rev. Lett.* **83**, 2085 (1999).
 - ³⁰D. N. Basov, E. J. Singley, and S. V. Dordevic, cond-mat/0103507.
 - ³¹The experimental data for simple metals like Cu, Au, or Ag are not available.
 - ³²J. Gonzalez, F. Guinea, and M. A. H. Vozmediano, *Phys. Rev. Lett.* **77**, 3589 (1996).
 - ³³P. W. Anderson, *Phys. Rev. B* **55**, 11 785 (1997).
 - ³⁴J. Edwards and R. F. Frindt, *J. Phys. Chem. Solids* **32**, 2217 (1971); S. F. Meyer, R. E. Howard, G. R. Stewart, J. V. Acrivos, and T. H. Geballe, *J. Chem. Phys.* **62**, 4411 (1975).
 - ³⁵The fact that the scattering rate differs *only* by a factor of ~ 2 for the two polarizations is somewhat surprising: because of the layered structure one intuitively expects charge carriers to have much more difficulties moving between than within the planes. Small anisotropy of $1/\tau(\omega)$ is another indication of good sample quality, since stacking of hexagonal NbSe₂ layers along c-direction must be nearly perfect.